Int. J. Electrochem. Sci., 11 **(2016)** 9123 – 9132, doi: 10.20964/2016.11.71

International Journal of ELECTROCHEMICAL SCIENCE
www.electrochemsci.org

The Electrochemical Performance of $LiMn_{1.96}Mg_{0.04}O_4$ Cathode Material Prepared by Solid-State Combustion Method

Lei Hu[1,2,3], *Miaomiao Shao*[1,2,3], *Junming Guo*[1,2,3,*], *Chang-wei Su*[1,2,3], *Jinhui Peng* [1,2,3,*]

[1] Key Laboratory of Comprehensive Utilization of Mineral Resources in Ethnic Regions, Yunnan Minzu University, Kunming 650500, *PR* China
[2] Key Laboratory of Resource Clean Conversion in Ethnic Regions, Education Department of Yunnan, Yunnan Minzu University, Kunming 650500, *PR* China
[3] Joint Research Centre for International Cross-border Ethnic Regions Biomass Clean Utilization in Yunnan, Yunnan Minzu University, Kunming 650500, PR China
[*]E-mail: guojunming@tsinghua.org.cn

Received: 23 July 2016 / *Accepted:* 19 July 2016 / *Published:* 10 October 2016

Mg-doped cathode materials $LiMn_{1.96}Mg_{0.04}O_4$ were synthesized at 500℃ for different calcining time by solid-state combustion method. The effects of calcining time on the crystal structure and microstructure were analyzed by scanning electron microcopy (SEM) and X-ray diffraction (XRD), the electrochemical properties were characterized by charge-discharge cycling test, cyclic voltammetry (CV) measurement and electrochemical impedance spectroscopy (EIS). The results showed that all samples demonstrated a single spinel structure; the crystal and the grain size grow up with the calcining time increasing. The $LiMn_{1.96}Mg_{0.04}O_4$ cathode calcined for 12 h had a high initial discharge specific capacity of 118.6 mAh g^{-1} and the best capacity retention was 93.00 % after 40 cycles at 0.2 C.

Keywords: Lithium-ion battery; $LiMn_{1.96}Mg_{0.04}O_4$; Electrochemical performance; cathode materials; solid-state combustion method

1. INTRODUCTION

Rechargeable lithium ions batteries (LIBs) are widely used as a favorable energy sources in telephones, hybrid electric vehicles (HEVs) and full electric vehicles (EVs). It is well know that spinel $LiMn_2O_4$ is the most promising positive electrode material due to its high energy density, low cost, low toxicity and environmental friendliness [1-5].However, because of the Jahn-Teller effect, the dissolution of manganese and decomposition of electrolyte solution at the electrode.$LiMn_2O_4$ suffers from low cycle life and poor rate performance, especially the rapid capacity fade at elevated temperature, which is a seriously obstacle for its large-scale commercial applications. To overcome these problems, the element doping is widely used to improve the structural stability and the cycle performance of $LiMn_2O_4$, such as Mg^{2+}[6]、Al^{3+}[7]、Cu^{2+}[8]、Fe^{2+}[9]、Ni^{2+}[10],which suppressed Jahn-Teller distortion and dissolution of Mn^{2+}.In addition, some researches demonstrated that the different preparation process for the spinel $LiMn_2O_4$ cathode material present the different electrochemical performance, such as sol-gel method [11], molten salt method [12], and hydrothermal synthesis [13].Among them, solid-state method is widely studied at present. Zhao et al. [14] reported that spinel $LiMn_2O_4$ was prepared by solid-state procedure, it exhibited a good cycling stability and rate capability good by a long heated time and high calcined temperature. Zhou et al. [14] reported that spinel $LiMn_2O_4$ was synthesized by solid-state combustion synthesis method which was calcined at a low reaction temperature and rapidly reaction rate due to an organic fuel mixed with raw materials. The fuel combustion released a large excess of heat, to accelerate the solid-state reaction rate.

In the previous work, $LiMn_{1.98}Mg_{0.02}O_4$ cathode materials were prepared by solid-state combustion method, mixed with citric acid at a rapid synthesis. Mg-doped $LiMn_{1.98}Mg_{0.02}O_4$ could be synthesized at a low reaction temperature [15]. In order to further study the high temperature performance, $LiMn_{1.96}Mg_{0.04}O_4$ cathode materials were prepared calcined at 500 ℃ for different time. The result shows that the cycling performances of Mg-doped $LiMn_{1.96}Mg_{0.04}O_4$ were obviously improved at high temperature with the increasing heat time. The influence of calcination time on Mg-doped $LiMn_2O_4$ materials, including rate capabilities and crystal structure, were also investigated in detail.

2. EXPERIMENTAL

2.1 Preparation of $LiMn_{1.96}Mg_{0.04}O_4$

$LiMn_{1.96}Mg_{0.04}O_4$ cathode materials were prepared by solid-state combustion synthesis. All of the reagents are analytically pure. stoichiometric ratio of Lithium carbonate, manganese carbonate and magnesium acetate(a total mixture mass of 30.0 g) were added in Teflon-lined jar,1.5 g citric acid as fuel and ethanol as medium were put in.The mixture was ball-milled thoroughly by planetary ball mill to make the raw materials dispersed homogeneously. The precursor mixture was off-white powder after drying at 80 ℃ in an oven. The precursor powder was put in an alumina crucible and calcined in a muffle furnace at 500 ℃ for 1, 3, 6, 9 h and 12 h in air atmosphere, respectively. The powder was obtained after cooling to room temperature.

2.2 Characterization of $LiMn_{1.96}Mg_{0.04}O_4$ Materials

The crystalline structure of the $LiMn_{1.96}Mg_{0.04}O_4$ samples was characterized by (X-ray diffraction (XRD，D/max-TTRⅢ,Japan) with Cu Kα radiation in 0.02 ^{o} step size, ranging from 10^{o} to 70^{o} at an operation current of 30 mA and voltage of 40 kV ,a scan speed was 4^{o} min^{-1})The morphology of the $LiMn_{1.96}Mg_{0.04}O_4$ powder was observed by scanning electron microscopy (SEM, QUANTA-200 American FEI Company).

2.3 Electrochemical Studies of $LiMn_{1.96}Mg_{0.04}O_4$ Materials

The cathodes were obtained by 80% active material, 10% polyvinylidene fluoride (PVDF) and 10%carbon black, dispersed in N-methyl-2-pyrrolidone (NMP) solvent followed by coating onto Al foil current collector and dried at 120 ℃in a vacuum oven for overnight. The coated Al foil was punched to obtained 16 mm diameter. Electrochemical performances were evaluated in coin cell (model CR-2025), which contained a working electrode and a lithium foil as counter electrode separated by a Celgard 2320 membrane. 1 $molL^{-1}LiPF_6$/EC+DMC+EMC (1:1:1 vol %) was used as the electrolyte. Electrochemical galvanostatical charge-discharge tests were performed by the Land electric test system CT2001A (Wuhan Jinnuo Electronic Co., Ltd).at 0.2 C between 3.20-4.35 V (vs. Li/Li^+). The cyclic voltammogram (CV) were measured on an electrochemical workstation (IM6ex, ZAHNER-elektrik GmbH＆Co. KG, Kronach, Germany) from 3.60 V to 4.50 V(vs. Li/Li^+) with a scan rate of 0.05 mVs^{-1}. Electrochemical impedance spectroscopy (EIS) was tested in the frequency range from 0.1 Hz to 100 KHz with an AC signal amplitude of 10 mV using the IM6ex electrochemical workstation.

3. RESULTS AND DISCUSSION

3.1 Structure and morphology

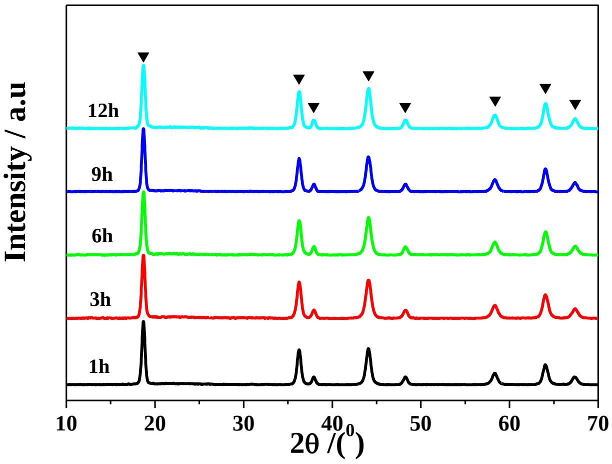

Figure 1. XRD patterns of $LiMn_{1.96}Mg_{0.04}O_4$ samples prepared at different calcination tempertures.

XRD patterns of $LiMn_{1.96}Mg_{0.04}O_4$ samples are presented in Fig.1 All of the materials prepared by solid-state combustion synthesis show a single spinel phase, which agreed with $LiMn_2O_4$ (JCPDS

No. 35-0782) [16]. This indicates that the doping-metal of Mg does not change the spinel structure of $LiMn_2O_4$. Eight typical peaks could be detected in Fig.1; from low angle to high angle is (111), (311), (222), (400), (331), (511), (440) and (531). The (400) peak slightly shifts to a high angle direction, the particle size tendency could be inferred by Bragg equation: $2d\sin\theta = n\cdot\lambda$ because of the lattice parameter will decrease, indicated a higher crystallinity and a better electrochemical performance, with the increase of calcination time.

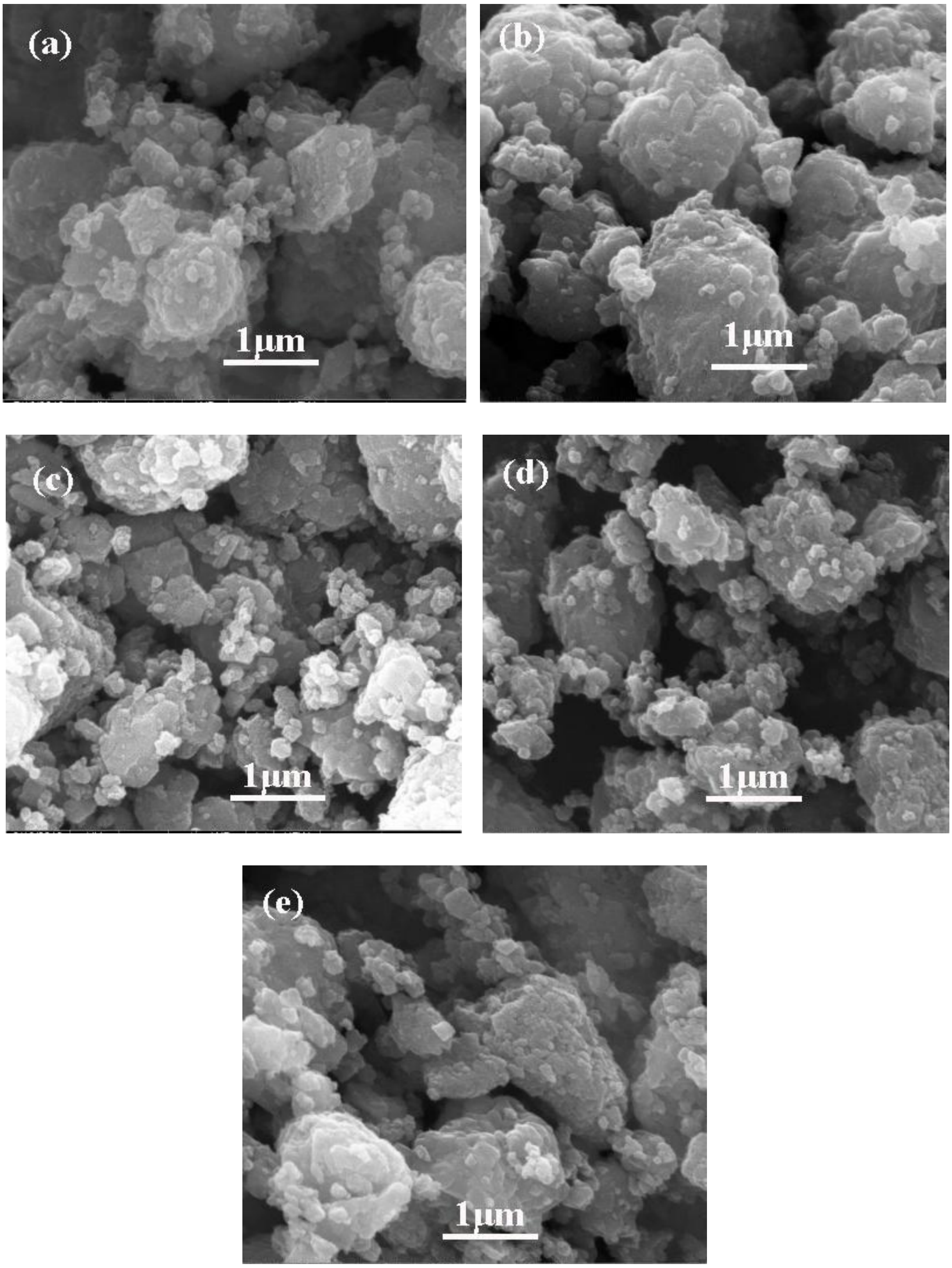

Figure 2. SEM images of $LiMn_{1.96}Mg_{0.04}O_4$ powders prepared at 500 ℃ calcined for a: 1 h, b: 3 h, c: 6 h, d: 9 h and e: 12 h.

Fig.2 displays the SEM images of the $LiMn_{1.96}Mg_{0.04}O_4$ calcined at different time show that all the sample powders are agglomerations that is composed of a small grain size, anging from 0.5-1.9um. The grain grow more completely, particle agglomerate seriously and maldistribution. However, with the increase of calcination time, the material of $LiMn_{1.96}Mg_{0.04}O_4$ for 9 h has a higher initial discharge specific capacity, which agreed with the minimun full width at half maximum FWHM in XRD, demonstrated a well-crystallinty.

3.2 Galvanostatic cycling

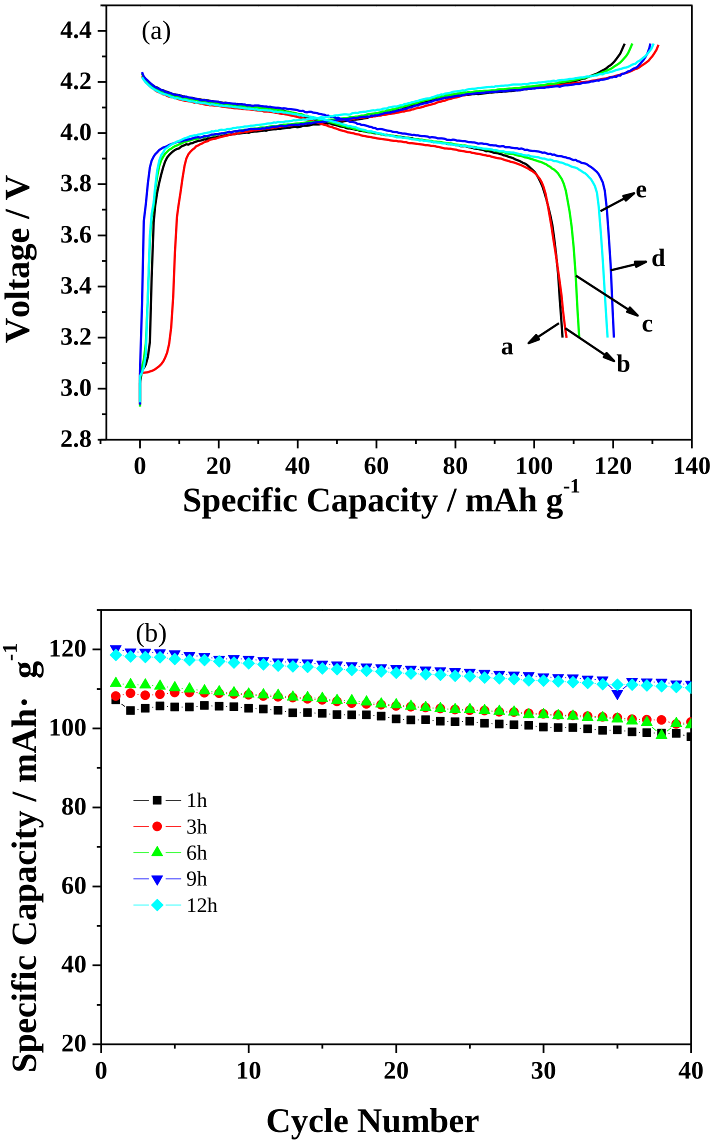

Figure 3. (a) Initial charge-discharge curves (a: 1 h, b: 3 h, c: 6 h, d: 9 h and e: 12 h), (b) Cycling performance of the $LiMn_{1.96}Mg_{0.04}O_4$ at 0.2 C rate.

The first charge-discharge curves of $LiMn_{1.96}Mg_{0.04}O_4$ prepared at different time are shown in Fig.3 (a) at 0.2 C rate between 3.20and 4.35V. All products delivery two evident potential at 3.90-4.20 V, which corresponds to that of the two-stage insertion/extraction during charge/discharge cyclic curves [17], implied that Mg-doping did not change the electrochemical reaction of lithium-ion during charge/discharge process [18]. Fig.3 (b) and Table 1 displays cycling performances tend to better after the increase of calcination time, the $LiMn_{1.96}Mg_{0.04}O_4$ caclined for 9 h show good discharge specific capacity and better capacity retentions, which shows a high initial discharge specific capacity of 118.6 mAh g^{-1} and the best capacity retentions of materials are 92.51%, suggesting that the cycle performance of $LiMn_{1.96}Mg_{0.04}O_4$ has been enhanced by the increased calcined time, which correspond with the structure stability exhibited in Fig.1

Table 1. Discharge specific capacity and capacity retention of $LiMn_{1.96}Mg_{0.04}O_4$ samples

Time（h）	Discharge specific capacity（mAh g^{-1}）		Capacity retentions (%)
	First	40th cycle	
1	107.2	97.9	91.32
3	108.2	101.6	93.90
6	111.4	100.9	90.57
9	120.2	111.2	92.51
12	118.6	110.3	93.00

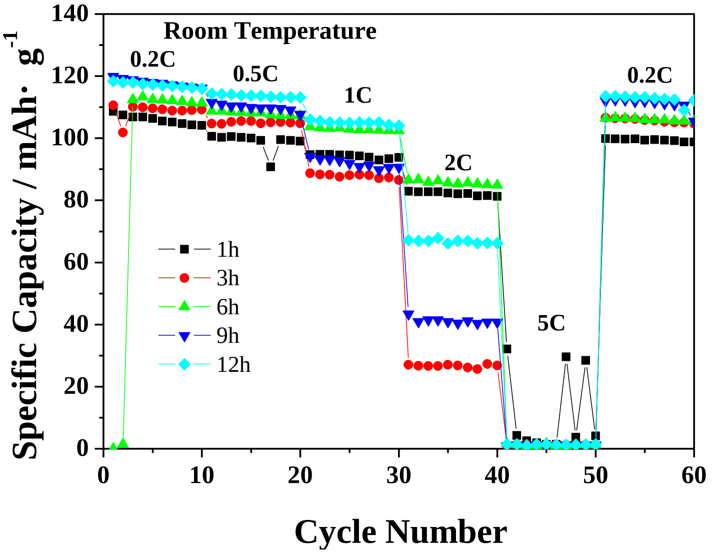

Figure 4. Discharge capacity vs. cycle number at various current rates from 0.2 C to 5 C (1 C=148 $mAhg^{-1}$) for $LiMg_{0.04}Mn_{1.96}O_4$

Fig.4 shows the C-rate capabilities of the $LiMg_{0.04}Mn_{1.96}O_4$ prepared at different timed. All the electrodes were measured in the voltage range of 3.20-4.35 V at various current rates from 0.5 C to 5 C

(1 C=148 mAh g^{-1}). It can be observed that the discharge capacity all decreases with the increasing of the discharge rate due to the low diffusion rate of the Li ions in the $LiMg_{0.04}Mn_{1.96}O_4$ particles. At 5 C, $LiMg_{0.04}Mn_{1.96}O_4$ prepared at 500 ℃ for 1 h delivered a discharge capacity of 29.6 mAh g^{-1}, while the other sample of different calcined time hardly discharged. The results indicate that the more calcined time that particle agglomerate seriously possessed high electrochemical polarization which delivered lower C-rate capabilities [19].

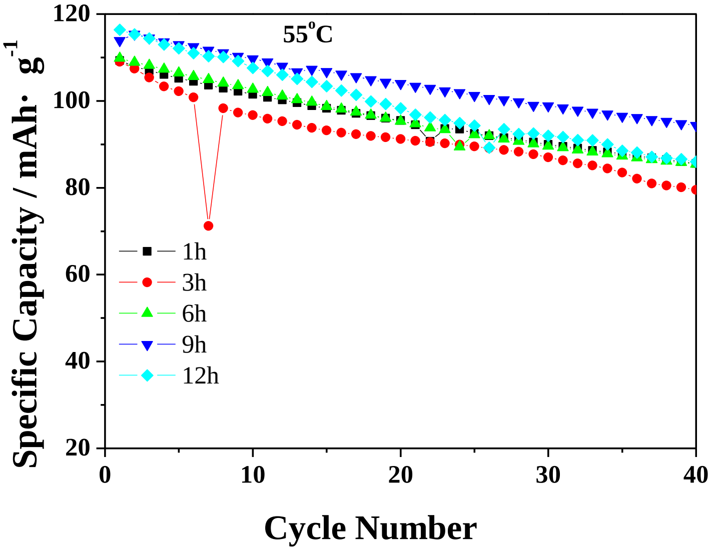

Figure 5. Cycle performance curves of $LiMg_{0.04}Mn_{1.96}O_4$ prepared at 500 ℃ for different calcining time at 0.2 C in the voltage range of 3.20-4.35 V at 55 ℃

Fig.5 shows cycle performance of the electrodes at 0.2 C between 3.20 and 4.35 V at 55 ℃. It can be found that the discharge capacity of $LiMg_{0.04}Mn_{1.96}O_4$ can be improved with the increase of calcination time at 55 ℃. $LiMg_{0.04}Mn_{1.96}O_4$ prepared at 500 ℃ for 9 h delivered a better discharge capacity compared with other electrodes. It shows the highest initial discharge specific capacity of 115.4 mAh g^{-1}, with the retentions of 92.51% after 40th cycles. It suggests that increasing the calcination time could improve the high temperature performance.

3.3 Cyclic voltammetry

Fig.6 shows the cyclic voltammograms of $LiMg_{0.04}Mn_{1.96}O_4$ materials prepared at 500℃ for different calcining time in the voltage range of 3.60-4.50 V and at a scan rate of 0.05 mVs^{-1}. There are two pairs of symmetrical redox peaks located at about 4.09 V/3.95 V and 4.23 V/4.10 V, which corresponded to the two potential plateaus in the charge/discharge curves from Fig.3 (a)implied that the two-stage intercalation/ deintercalation process of Li ions in lithium-ion[20], further indicating Mg-substitution does not change severely the redox potentials of $LiMn_2O_4$[21].

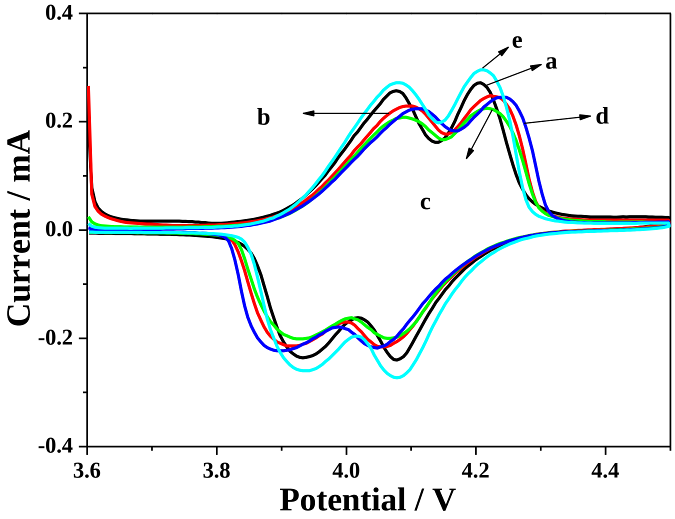

Figure 6. Cyclic voltammogram curves of the $LiMg_{0.04}Mn_{1.96}O_4$ samples following calcinations time (a: 1 h, b: 3 h, c: 6 h, d: 9 h and e: 12 h)

There is no obvious trend changes for peak current and peak area, while, that of sample prepared with the increasing of clacination time, the differences in potential between the anodic and cathoodic peaks are decreased and a well-defined splitting and symmetric could be observed[22], which indicated a better reversibility and capacity retention, it agreed with the result from Table 1.Although, the crystallinity and symmetry of $LiMg_{0.04}Mn_{1.96}O_4$ were improved, that particle agglomerate, which reduced the Li+ ion diffusion rate in the charge/discharge process, resulting in reducing the electrochemical activity, it is not beneficial to the high rate performance[23]

However, with the increasing of clacination time, the capacity rention could effectively improved, further more that $LiMg_{0.04}Mn_{1.96}O_4$ calcined for 9 h displays a high initial discharge specific capacity and a best capacity retention.

3.4 Electrochemical impedance spectroscopy

Fig.7 presents the Nyquist plots of $LiMg_{0.04}Mn_{1.96}O_4$ samples at 500 ℃ for 1 h, 3 h, 6 h, 9 h and 12 h after 10 charge-discharge cycles. The impedance spectra consist of a semicircle in the middle-high frequency (HZ) region and a slope in the low frequency region. An intercept in the high-frequency region of the Z_{rel} axis indicates the ohmic resistance (R_s); the semicircle is related to the charge transfer resistance (R_{ct}), the constant phase element (CPE) represents the capacitance of the double layer, the slope in the low frequency region corresponds to Warburg impedance (W). It is known that the cell impendence is mainly attributed to R_{ct}. The lower R_{ct} implied the lower kinetic resistance, lower polarization and higher lithium-ion diffusibility during electrochemical reaction. It is evident that the sample calcined for 12 h exhibited a lower R_{ct} with the extend of clacination time, which is consistent with the tendency in CVs and the electrochemical performance in Fig.3

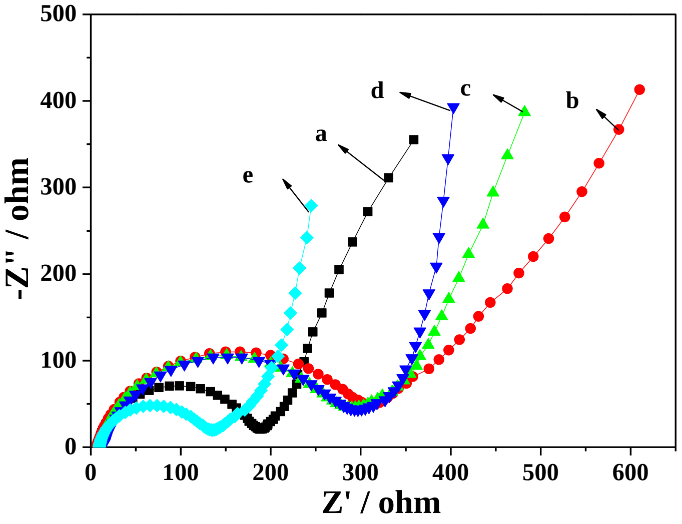

Figure 7. Nyquist plots of $LiMg_{0.04}Mn_{1.96}O_4$ materials at 500 ℃ for a: 1 h, b: 3 h, c: 6 h, d: 9 h and e: 12 h

4. CONCLUSIONS

The main crystalline phase of $LiMg_{0.04}Mn_{1.96}O_4$ materials were prepared at 500 ℃ for calcining various time by a solid-state combustion synthesis. The crystallinity of the materials was improved, while that showing a better electrochemical performance, with the increase of calcination time. The $LiMg_{0.04}Mn_{1.96}O_4$ materials were prepared for calcination time of 12 h exhibits a good electrochemical performance with initial discharge specific discharge capacity of 118.6mAh g^{-1} and maintains of 93% of initial discharge after 40 cycles at 0.2C..

ACKNOWLEDGEMENTS

This work was financially supported by the National Natural Science Foundation of China (51262031, 51462036), Program for Innovative Research Team (in Science and Technology) in University of Yunnan Province (2011UY09), Yunnan Provincial Innovation Team (2011HC008), and Innovation Program of Yunnan Minzu University (2016TX09).

References

1. X.Q. Wang, J. Wang, J.W. Wu, B.W. Cheng, M.B. Ma and Z.Z. Jiang, *Ionics* 21 (2015) 851–1856.
2. X.Q. Wang, O. Tanaike, M. Kodama and H. Hatori, *Journal of Power Sources* 168 (2007) 282–287.
3. H.Y. Zhao, X.Q. Liu, C. Cheng, Q. Li, Z. Zhang , Y. Wu , B. Chen and W.Q. Xiong, *Journal of Power Sources* 282 (2015) 118-128.
4. Y.J. Cai, Y.D. Huang, X.C. Wang, D.Z Jia, W.K. Pang, Z.P. Guo, Y.P. Du and X.C. Tang, *Journal of Power Sources* 278 (2015) 574-581.

5. D.L. Guo, B. Li, Z.R. Chang, H.W. Tang, X.H. Xu, K. Chang, E. Shangguan, X.Z. Yuan and H.J. Wang, *Electrochimica Acta* 134 (2014) 338–346.
6. H. Zhang, D. Liu, X.S. Zhang, C.J. Zhao and Y.L. Xu, *J Solid State Electrochem* 18 (2014) 569–575.
7. X. Yi, X.Y. Wang, B.W. Ju, Q.L. Wei, X.K. Yang, G.S. Zou, H.B. Shu and L. Hu, *Journal of Alloys and Compounds* 604 (2014) 50–56.
8. B. Ebin, S. Gürmen and G. Lindbergh, *Materials Chemistry and Physics* 136 (2012) 424-430.
9. H.Q. Liu, R.Y. Tian, Y. Jiang, X.H. Tan, J.K. Chen, L. Zhang, Y.J. Guo, H.F. Wang, L.F. Sun and W.G. Chu, *Electrochimica Acta* 180 (2015) 138–146.
10. L.F. Xiao, Y.Q. Zhao, Y.Y. Yang, X.P. Ai, H.X.Yang and Y.L. Cao, *J Solid State Electrochem* 12 (2008) 687-691.
11. C.L. Chen, K.F. Chiu, Y.R. Chen , C.C. Chen , H.C. Lin and H.Y. Chiang , *Thin Solid Films* 544 (2013) 182-185.
12. M. Helan, L.J. Berchmans, T. P. Jose, A. Visuvasam, S. Angappan, *Materials Chemistry and Physics* 124 (2010) 439-442.
13. B.K. Zou, X.H. Ma, Z.F. Tang, C.X. Ding, Z.Y. Wen and C.H. Chen, *Journal of Power Sources* 268 (2014) 491-497.
14. X.Y. Zhou, M.M. Chen, M.W. Xiang, H.L. Bai and J.M. Guo, *Ceramics International* 39 (2013) 4783–4789.
15. M.W. Xiang, C.W. Su, L.L. Feng, M.L. Yuan and J.M. Guo, *Electrochimica Acta* 125 (2014) 524–529.
16. H.Y.Zhao, F.Li, X.Q.Liu, C.Cheng, Z.Zhang, Y.Wu, W.Q.X, B.Chen, *Electrochimica Acta* 151(2015)263-269
17. H.Y. Zhao, S.S. Liu, Y. Cai, Z.W. Wang, M. Tan and X.Q. Liu, *Journal of Alloys and Compounds* 671 (2016) 304-311.
18. H.Y. Zhao, S.S. Liu, Z.W. Wang, Y. Cai, M. Tan and X.Q. Liu, *Electrochimica Acta* 199 (2016) 18–26.
19. Y.H. Wang, L. Chen, Y.G. Wang and Y.Y. Xia, *Electrochimica Acta* 173 (2015) 178–183.
20. B.M. Hwang, S.J. Kim, Y.W. Lee, H.C. Park, D.M. Kim and K.W. Park, *Materials Chemistry and Physics* 158 (2015) 138-143.
21. M.Prabu, M.V.Reddy, S.Selvasekarapandian, G.V.Subba Rao and B.V.R.Chowdari, *Electrochimica Acta*,88(2013)745
22. X.N. Ding, H.W. Zhou, G.C. Liu, Z. Yin, Y. Jiang and X.D. Wang, *Journal of Alloys and Compounds* 632 (2015) 147–151.
23. C.H. Jiang, S.X. Dou, H.K. Liu, M. Ichihara and H.S. Zhou, *Journal of Power Sources* 172 (2007) 410–415.